PHYSICAL REVIEW B VOLUME 40, NUMBER 9 15 SEPTEMBER 1989-II

Raman scattering determination of structures for SiC polytypes: Quantitative evaluation with a revised model of lattice dynamics

S. Nakashima and K. Tahara
Department of Applied Physics, Osaka University, Yamadaoka, Suita, Osaka 565, Japan

(Received 22 May 1989)

Quantitative structural analysis by measurements of Raman intensity profiles has been undertaken for silicon carbide (SiC) polytypes. Since the Raman intensity is sensitive to the choice of atomic displacements, previous models of lattice dynamics are reexamined. Force-constant parameters of a linear-chain model are determined so that calculated phonon dispersions and Raman intensity profiles fit the experimental results. The Raman intensity profiles calculated using these force constants agree quantitatively with the observed spectra for a number of polytypes. This agreement indicates that the set of the force constants thus determined can commonly be used for any polytypes of SiC and also that the bond polarizability concept is applicable to folded modes of both the acoustic and optical branches.

I. INTRODUCTION

Silicon carbide (SiC) is known to have a large number of polytypes.[1] The building units of SiC structures are double layers of Si and C atoms with the polytypes differing in the stacking order of the double layers. The short-range structure is simple, a fourfold-coordinated diamondlike arrangement of alternate C and Si atoms. For the wurtzite structure, all double layers occur in a hexagonal environment, and for the cubic structure (3*C* type) all double layers occur in a cubic environment. Other higher-order polytypes are constructed from a mixture of hexagonal and cubic double layers.

Until now, the crystal structures of SiC polytypes have been determined mainly through x-ray and electron-microscope analyses. Recent Raman scattering studies[2,3] have demonstrated that a Raman-intensity analysis is also useful in identifying the polytype structure of $\mathrm{CdI_2}$ as well as SiC. Long-period SiC polytypes, which form superlattices with a homostructure, are compared to artificial superlattices having a heterostructure. Raman spectra of SiC polytypes exhibit a number of folded modes arising from the transverse-acoustic (TA) and -optical (TO) branches.[3-5] The intensity profiles of these folded modes provide us with information on the stacking structure of the Si and C planes as does the x-ray-intensity analysis.

The folded modes reflect the periodicity and symmetry of the crystals, since they arise from the Bragg reflection of phonons having wave vectors corresponding to Brillouin-zone (BZ) boundaries.

The relative intensity of the folded modes has been analyzed by a model based on the bond-polarizability concept.[3,6] In this model, Raman polarizability tensors are obtained as the sum of the contributions from bond Raman polarizabilities multiplied by the bond-length variation. For SiC polytypes, the bond Raman polarizabilities can be approximately expressed by a single parameter for the folded TA and TO modes. Accordingly, the Raman scattering intensity distribution depends only on the atomic displacements.

In a previous paper Raman scattering profiles were analyzed using a linear-chain model in which the two nearest-neighbor force constants were involved and the difference between the forces in cubic and hexagonal stackings were taken into account.[3,7] Qualitative agreement was obtained between calculated and experimental intensity profiles of the folded TA and TO modes in 6*H*, 8*H*, 15*R*, and 21*R* polytypes. However, noticeable discrepancies between the experimental and theoretical results were observed for several points. First, the calculated intensity profiles for the folded TO modes of the 27*R* and 15*R* polytypes were quite different from those observed.[3,7] Second, the calculated intensity ratios of the folded modes of the TO and TA branches were different from those measured. The calculated intensity profile reproduced the observed spectrum of the folded mode for each branch. However, the calculated intensity ratio, e.g., for the strongest folded modes in the TA and TO branches, was about 10 times as large as the observed ratio. Third, the calculated intensity for the weak partner of a doublet of the folded TA mode was weak compared with the observed one.

Several models of lattice dynamics were examined to remove these discrepancies within the framework of the zinc-blende–structure approximation.[8] However, no appreciable improvement as to the explanation of the intensity ratio was found, although some models explain rather well the phonon dispersion relations of TA and TO branches in the Γ-*L* direction.

In this work the intensity profiles of the folded mode are reexamined in the framework of a linear-chain model using short-range force constants extended to the third neighbors and taking into account the force difference between cubic and hexagonal environments. The force constants are usually determined so as to reproduce only the phonon dispersion curves. However, in this work, the force constants are calculated in such a way that they explain not only the experimental phonon dispersions but also Raman intensity profiles.

Recently, it has been found that the relative intensity of partners in the doublet of folded TA modes depends strongly on the scattering wave vector q[9]. This result indicates that Raman intensity profiles of SiC polytypes observed with a backscattering geometry should be compared with the results calculated for finite scattering wave vectors. The q dependence of the Raman intensity profiles will be described in the following article (hereafter referred to as II).

Using the linear-chain model and the force constants thus determined, Raman intensity profiles are calculated for various polytypes with finite-scattering wave vectors. The calculated intensity profiles agree quantitatively with the observed spectra of polytypes examined to this point. The most important fact is that the set of force constants determined is common to all SiC polytypes and can be used for identification of any polytype structure.

II. THEORETICAL BACKGROUND

The Raman scattering intensity for phonon modes at the Γ point is proportional to the square of the Raman polarizability tensor. The Raman tensor consists of contributions from constituent bonds in a unit cell. They are expressed by the bond Raman polarizability multiplied by the relative displacement of the end atoms relevant to the bond. For the folded modes of transverse-optic and -acoustic branches in SiC, the bonds tilted against the c axis[2] (e.g., α—B, β—C, and γ—A) contribute to the Raman tensors, while there is no contribution from the bonds parallel to the c axis (α—A, β—B, and γ—C bonds). Here, the Latin letters A,B,C and Greek letters α, β,γ represent the positions of silicon and carbon atoms, respectively. The components of the bond Raman polarizability tensor which arise from the former group of bonds can be expressed by a single parameter. The wave vectors of phonons transferred from photons with a backscattering geometry cannot always be regarded as negligible. Such a finite-q effect for the intensity of the folded TA modes has been demonstrated in II. The Raman tensor components of the λth transverse folded modes with a finite q is given by Eq. (12) of II as

$$\alpha_{\rho\sigma}^{(\lambda)}(q)=c\sum_{j}\pm[u^{(\lambda)}(j)-u^{(\lambda)}(j+1)]\exp(iqz_j)\ , \tag{1}$$

where c is the xy component of the Raman polarizability tensor. The signs in the above equation depend on the type of bonds. A plus sign is assigned to the group of bonds (a) α—B, β—C, and γ—A, and minus sign for the group of bonds (b) α—C, β—A, and γ—B or vice versa. $[u(j)-u(j+1)]$ is the relative displacement of the end atomic planes of the bonds tilted against the c axis and z_j is the central position of the bond along the c axis. When setting $q=0$, Eq. 1 is reduced to Eq. (19) of Ref. 3. The Raman scattering intensity for the λth mode is given by

$$W_\lambda=S\frac{n(\omega_\lambda)+1}{\omega_\lambda}|\mathbf{e}_i\alpha_{\rho\sigma}^{(\lambda)}\mathbf{e}_s|^2\ , \tag{2}$$

where S is a constant independent of ω, $n(\omega)$ is the Bose factor, and $\mathbf{e}_i$ ($\mathbf{e}_s$) is the polarization vector of the incident (scattered) light. The magnitude of the scattering wave vector q is given by $q=4\pi n/\lambda$ for the backscattering geometry, where λ is the wavelength of the light and n is the refractive index, given as 2.69 for SiC. The value of qc is 0.017 at 4880 Å, where c is the unit-cell length along the [111] direction of the $3C$ polytype.

The displacement amplitudes of the atomic planes are obtained by solving the equations of motion. In this work use is made of a linear-chain model,

$$\begin{aligned}M_j\omega^2u(n|j)&=\sum_{r,s}K_{j,j+s}^{r}[u(n|j)-u(n+r|j+s)]\\&=\sum_{r,s}D_{j,j+s}^{r}u(n+r|j+s)\ ,\end{aligned} \tag{3}$$

where $u(n|j)$ and M_j are the displacement and mass of the jth rigid plane in the nth unit cell, respectively, and $D_{j,j+s}^{r}$ is the interplanar force. The displacement $u(n|j)$ is expressed as

$$u(n|j)=u(j)\exp(-iqx_n) \tag{4}$$

and

$$u(j)=A_j\exp\{i[-qx_j+\phi_j(q)+\alpha(q)]\}\ . \tag{5}$$

The frequency of the phonon modes is determined from the secular equation,

$$|M_j\delta_{ij}\omega^2-D_{ij}(q)|=0\ , \tag{6}$$

where

$$D_{ij}(q)=\exp[-iq(x_j-x_i)]\sum_{n}D_{i,j}^{n}\exp(-iqx_n)\ . \tag{7}$$

The linear chain of atomic planes along the [111] direction for the $6H$ polytype is displayed schematically in Fig. 1, together with the forces connecting them. In this

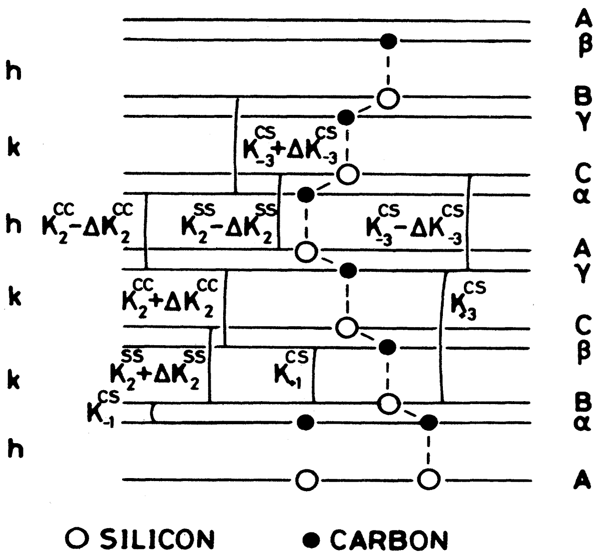

FIG. 1. Parallel planes of silicon and carbon atoms along the [111] direction, representing a linear-chain model. The force connecting atomic planes K_n corresponds to the interplanar force $K_{j,j+n}$ in Eq. (3). The superscript of the force-constant "SiC" is affixed to the odd-neighbor interaction.

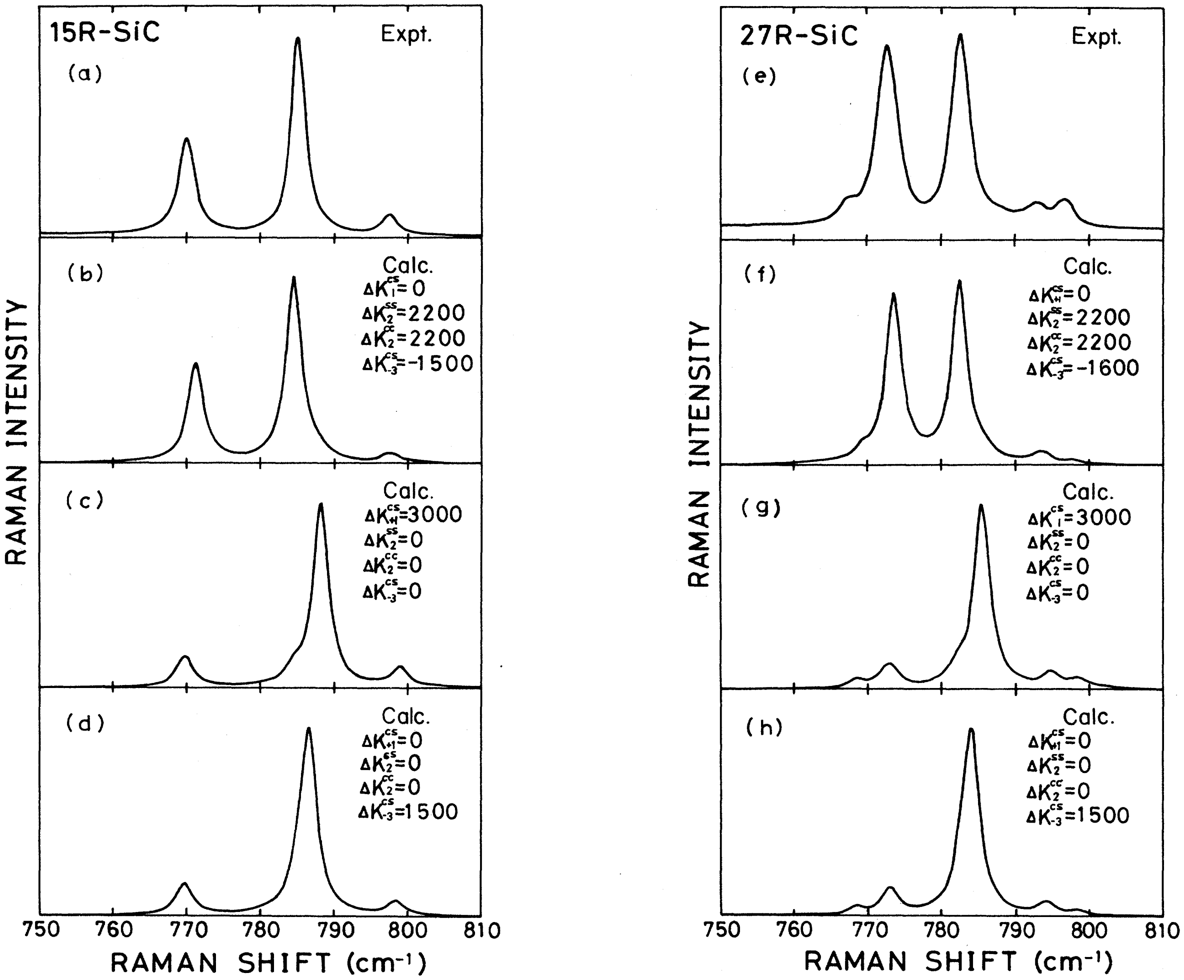

FIG. 2. Observed Raman spectra of the folded TO modes for (a) 15*R* and (e) 27*R*. Raman intensity profiles are calculated for different force-constant parameters in (b)–(d) and (f)–(h). The force constants other than those shown in the figures ($k_{-1}-k_{+3}$) are given in Table I. The Raman bands are drawn by assuming Lorentzian band shape with a full width at half maximum (FWHM) of 2.6 cm^{-1}.

model the interplanar forces are taken into account up to the third-neighbor plane. The stacking sequence of the 6*H* polytype is expressed by $(hkk)_2$ in the *hkk* notation or *ABCACB* in the *ABC* notation. It is assumed that the nearest-neighbor plane forces K^{cs}_{-1} and K^{cs}_{+1} and the third-neighbor force K^{cs}_{+3} are independent of the stacking, whereas the second- and third-neighbor plane forces depend on the stacking. For the cubic configuration, they are $K_i+\Delta K_i$, while for the hexagonal configuration, $K_i-\Delta K_i$. Although this figure is shown for the 6*H* polytype, the basic concept is applied to all other polytypes.

The force constants are determined by the following procedure. First, the force constants $K^{cs}_{-1}-K^{cs}_{+3}$ are determined so that the calculated dispersion curves approximately reproduce those experimentally determined. Since all six parameters are not determined independently in this fitting procedure, a restriction is imposed such that $K^{ss}_2/M=K^{cc}_2/m$ for convenience, where M and m are the masses of Si and C atoms, respectively. The values of K^{cs}_{-1} and K^{cs}_{+1} are determined under the condition that K^{cs}_{-1} and $K^{cs}_{-1}-K^{cs}_{+1}$ become very small. This requirement arises from the fact that in the force-constant models in Ref. 3, the relative displacement of the end atoms for the bond relevant to the force constant K^{cs}_{-1} is small. Also, the intensity ratios of folded TO and TA modes are much larger than those observed.

TABLE I. The force-constant parameters used in the linear-chain model shown in Fig. 1. These values were determined by fitting of the frequency and intensity of the Raman bands. Values are in units of 10^4 dyn/cm.

k^{cs}_{-1}	k^{cs}_{+1}	k^{ss}_{2}	k^{cc}_{2}	k^{cs}_{-3}	k^{cs}_{+3}	Δk^{ss}_{2}	Δk^{cc}_{2}	Δk^{cs}_{-3}
27.3	5.38	0.493	0.211	−1.81	0.717	0.22	0.22	−0.16

In the determination of the ΔK_i, the following experimental results were noted: (1) the folded TO mode in the $2H$ polytype is 762 cm^{-1}, which is smaller than the value of the corresponding mode in the $6H$ polytype (768 cm^{-1}), and (2) the frequency of the observed folded TO mode with $q(\frac{1}{2})$ in the $4H$ polytype (776 cm^{-1}) is lower than the frequency calculated using the determined force constants $K^{cs}_{-1} \sim K^{cs}_{+3}$. The folded mode corresponding to the phonon mode at q in the Brillouin zone of the $3C$ polytype is denoted as the $q(x)$ mode hereafter, where $x=q/q_B$, $q_B=\pi/c$. The latter fact suggests that the observed mode at 776 cm^{-1} is a low-frequency counterpart of a widely separated doublet. Taking finite values of ΔK^{ss} and ΔK^{cc}_{2} alters the frequencies of the $q(x\neq0)$ mode, but not that of the $q(0)$ mode. It gives a relatively large splitting (6 cm^{-1}) to the $q(\frac{1}{2})$ doublet of the $4H$ polytype which has a strong low-frequency component. Also, it reproduces the intensity profiles of the folded TO modes for the $15R$ and $27R$ polytypes. The ΔK^{cs}_{-3} is set negative in order to obtain agreement between the calculated splitting of the folded TA doublets and observed values.

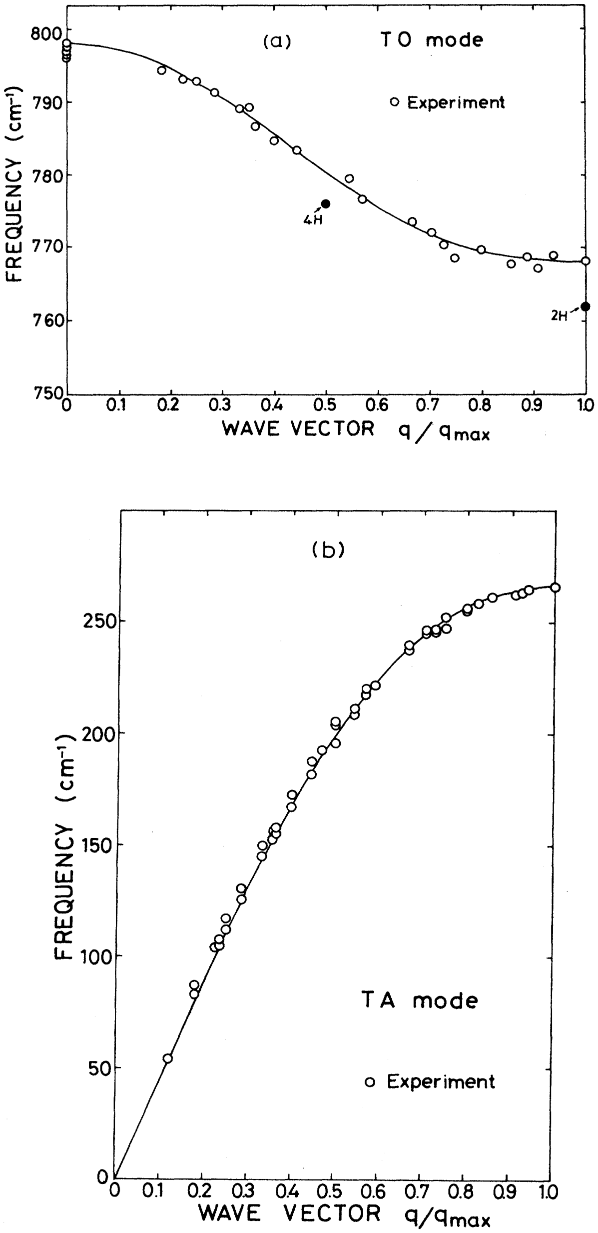

FIG. 3. Phonon dispersion curve of (a) TO branch and (b) TA branch of the $3C$ polytype, which is deduced from the frequencies of the folded modes of various polytypes. The solid circles are the experimental values for the $2H$ and $4H$ polytypes. The solid line is the dispersion calculated using the force-constant parameters in Table I, with $\Delta K_i=0$.

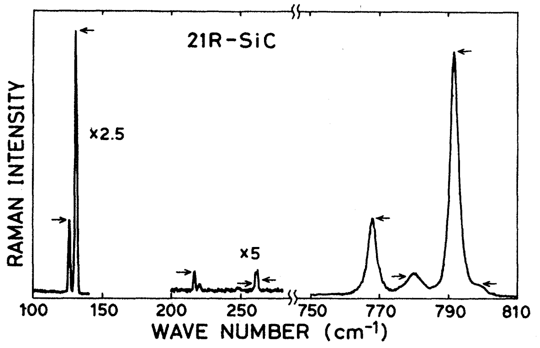

FIG. 4. Raman intensity profile of the $21R$ polytype measured with a backscattering geometry. The horizontal bars indicate the calculated intensities.

Figure 2 shows the calculated intensity profiles of folded TO modes in the $15R$ and $27R$ polytypes for different values of ΔK_i when the values of the other force constants $(K^{cs}_{-1}-K^{cs}_{+3})$ are fixed. Although the frequency changes slightly, the Raman intensity profiles change drastically with ΔK_i. The values of ΔK_i shown in Figs. 2(b) and 2(f) provide the best fit to the observed spectra shown in Figs. 2(a) and 2(e). The force constants determined by fitting the experimental and calculated results for dispersion curves and intensity profiles are listed in Table I.

III. COMPARISON WITH EXPERIMENTAL RESULTS

The Raman spectra of SiC polytypes have been measured in a backscattering geometry using the 4880-Å line of an Ar$^+$-ion laser. Thin crystal platelets having (0001) faces were examined. In this scattering geometry the xy component of the Raman polarizability tensor is observed for the folded TO and TA modes.

A folded mode with $q=0$ in long-period polytypes corresponds to a phonon mode in the basic polytype (zinc-blende structure). Accordingly, the phonon dispersion curves in the basic BZ are reduced from the frequencies of the folded modes in long-period polytypes if their frequencies are not much affected by the stacking arrangement. Figures 3(a) and 3(b) show the frequencies of folded modes of various polytypes up to $51R$, which are represented in the form of dispersion curves in the basic BZ. The solid lines are calculated from the model of lat-

TABLE II. Comparison between calculated and measured Raman intensities of the folded modes. The Raman intensity is normalized in such a way that the intensity of the strongest band of each branch is unity. Calc. (1) and Calc. (2) are the results of the present work and of Ref. 3, respectively.

		Folded TO mode				Folded TA mode			
		Frequency Expt.	Intensity			Frequency Expt.	Intensity		
Polytype	$x=q/q_B$	(cm^{-1})	Expt.	Calc. (1)	Calc. (2)	(cm^{-1})	Expt.	Calc. (1)	Calc. (2)
15*R*	0	798	<0.08	0.04	0.13				
	0.4	786	1.0	1.0	1.0	167	0.15	0.15	0.08
						173	1.0	1.0	1.0
	0.6	770	0.49	0.51	0.17	254	0.08	0.03	0.038
						256	0.04	0.01	0.034
6*H*	0	798	0	0	0				
	0.33	789	1.0	1.0	1.0	144	0.17	0.19	0.04
						150	1.0	1.0	1.0
	0.66	0	0	0	0		0	0	0
						240	0.014	0	0
	1.0	768	0.3	0.33	0.22	266	0.06	0.01	0.05
21*R*	0	797	0.03	0.02	0.07				
	0.28	792	1.0	1.0	1.0	126	0.29	0.32	0.035
						131	1.0	1.0	1.0
	0.57	779	0.065	0.06	0.06	216	0.03	0.04	0.04
						219	0.004	0.007	0.01
	0.86	768	0.31	0.32	0.16	260	0.02	0.01	0.03
						261	0.03	0.014	0.015

tice dynamics in which the forces are assumed to be independent of the stacking arrangement, i.e., $\Delta K_i=0$. The calculated result reproduces rather well the experimental dispersions with the exception of a few points.

It should be noted that the frequency of the $q(\frac{1}{2})$ mode in the TO branch for the 4*H* polytype deviates appreciably from the calculated dispersion curve. This may be due to the fact that the splitting of the $q(\frac{1}{2})$ doublet for the 4*H* polytype is large and the Raman intensity is much larger for the low-frequency than for the high-frequency partner. Such a deviation from the calculated dispersion curve is also found for the $q(1)$ mode of the TO branch in the 2*H* polytype. The frequencies calculated using the force constants in Table I show fair agreement with the observed frequencies for the 2*H* and 4*H* polytypes. These results indicate that the stacking dependence of interatomic interactions is important for the 4*H* and 2*H* polytypes for which the percentage of hexagonal planes in the polytype arrangement is large.

The observed Raman intensity profiles are compared with calculated values (shown by horizontal bars) in Fig. 4 for the 21*R* polytype and are listed in Table II. It can be seen that quantitative agreement exists between the observed and calculated results for the folded TO modes of these polytypes. There are disagreements for the weak folded modes of the TA branch with $x=1$. Calculated intensity profiles for many other polytypes lower than the 66*R* polytypes were compared with the observed spectra,

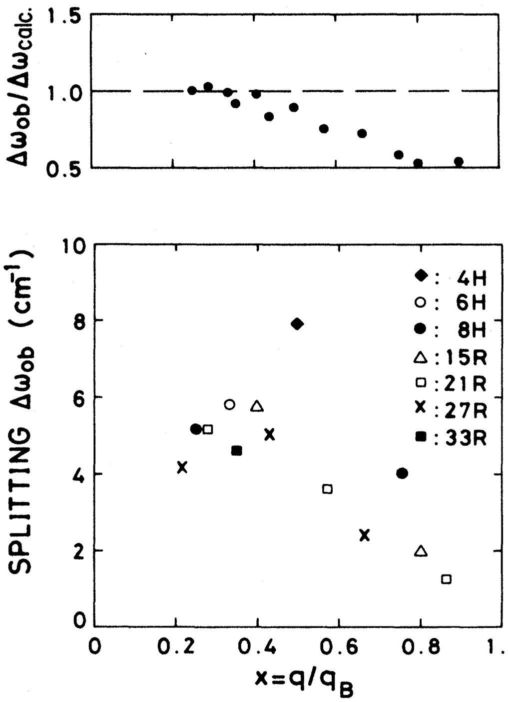

FIG. 5. The splitting of the doublets for folded TA modes vs reduced wave vector x. The ratio of the observed splitting to calculated splitting is also plotted as a function of x.

although the results are not shown here. Excellent agreement was obtained, especially for the folded TO modes. Discrepancies are observed in some weak folded modes of the TA branch of higher polytypes. This is partly due to the fact that these higher polytypes usually contain a disorder.

The validity of the lattice-dynamics model is further supported by examination of the intensity ratio of the folded TO and TA modes. In Table III a comparison is made of the calculated and experimental ratio for the most intense folded modes of each branch. The experimental values are taken from the data measured in the backscattering configuration. As can be seen in Table III, the calculated result is in agreement with the observed ratio of the integrated intensity. The results calculated by using several models in which interatomic interactions are assumed to be independent of the stacking arrangement do not coincide with the observed ratio.[8] The results shown in Table III demonstrate that the same Raman polarizability can be used in common with the folded TO and TA modes.

Another test for the validity of the model is the frequency splitting of the doublets for the folded TA modes and the intensity ratio of the low- and high-frequency components. The q dependence of the splitting and intensity ratio for the doublets has been examined in II. Excellent agreement was found between experimental and calculated values for the above quantities.

Frequency splitting of the folded TA modes was discussed by Feldman *et al.*[5] and Hodges.[10] Hodges calculated the splitting by a perturbation method. Assuming that Si-C double planes separated by $(\frac{1}{4})c$ move as rigid bodies for the acoustic branches and using a linear-chain model along with a shell model, he derived an expression for the splitting. The theoretical splitting obtained using the shell model was related to structure factors $S(2q)$, $S(0)$, and $[\sin(\frac{1}{2}qc)]^2$, where q is the wave vector of a phonon in the basic BZ corresponding to the folded mode. However, the agreement with experimental splitting was not satisfactory.

The splitting was calculated by use of the present model. Figure 5 shows the measured splitting frequency of the doublets for various polytypes. The ratio of the observed splitting to the calculated value is also plotted against $x = q/q_B$. The ratio is almost unity, for $x \leq 0.5$, but deviates systematically from unity as x increases. This result suggests that the inclusion of interplanar forces between the more distant separated planes is necessary to reproduce the observed splitting with the model.

TABLE III. Raman intensity ratios of the folded TO and TA modes. The ratios were measured at 4880 Å.

Polytype	$x = q/q_B$	I_{TO}/I_{TA} (expt.)	(calc.)
6H	$\frac{1}{3}$	7.6	7.7
15R	$\frac{2}{5}$	6.4	7.3
21R	$\frac{2}{7}$	6.8	8.4

IV. CONCLUSIONS

Raman intensity profiles in SiC polytypes have been examined using a revised lattice-dynamics model and the bond-polarizability concept. In this model the force-constant parameters were determined so that the experimental dispersion curves and Raman intensity profiles agree with those observed. In a number of polytypes examined to date, quantitative agreement between the calculated and observed profiles has been obtained for the folded modes of the TO and TA branches. This indicates that the Raman intensity analysis can be used to identify the stacking structure of SiC polytypes such as that used in x-ray-diffraction analysis.

The lattice-dynamics model used takes the third-neighbor plane forces into account and also the difference between the forces in hexagonal and cubic configurations. It was found that the intensity of certain folded TO modes and the intensity ratio of the folded modes for the TO and TA branches were sensitive to this force difference. This finding indicates that the Raman intensity analysis can also be used to check the validity of the vibrational amplitudes of atoms. In the present model it is not necessary to use different Raman polarizabilities for the folded TO and TA modes.

At the present time it is not clear that the force constants determined in this work are a unique solution. However, the quantitative agreement between the observed and calculated spectra demonstrated that the set of force constants determined in this work is common to all polytype structures and that these force constants are applicable in the determination of the structure of unknown higher polytypes.

---

[1] A. R. Verma and P. Krishna, *Polymorphism and Polytypism in Crystals* (Wiley, New York, 1966).

[2] S. Nakashima, H. Katahama, Y. Nakakura, and A. Mitsuishi, Phys. Rev. B **31**, 6531 (1985).

[3] S. Nakashima, H. Katahama, Y. Nakakura, and A. Mitsuishi, Phys. Rev. B **33**, 5721 (1986).

[4] D. W. Feldman, J. H. Parker, Jr., W. J. Choyke, and L. Patrick, Phys. Rev. **170**, 698 (1968).

[5] D. W. Feldman, J. H. Parker, Jr., W. J. Choyke, and L. Patrick, Phys. Rev. **173**, 787 (1968).

[6] S. Nakashima and M. Balkanski, Phys. Rev. B **34**, 5801 (1986).

[7] S. Nakashima, Y. Nakakura, and Z. Inoue, J. Phys. Soc. Jpn. **56**, 359 (1987).

[8] S. Nakashima, Y. Nakakura, A. Wada, and K. Kunc, J. Phys. Soc. Jpn. **57**, 3828 (1988).

[9] S. Nakashima and T. Tahara, in *Proceedings of the 11th International Conference on Raman Spectroscopy, London, 1988,* edited by R. J. H. Clark and D. A. Long (Wiley, New York, 1988), p. 333.

[10] C. H. Hodges, Phys. Rev. **187**, 994 (1969).